

Regional amplification of ground motion in central Mexico. Results from coda-length magnitude data and preliminary modeling

Martín Cárdenas¹, Francisco J. Chávez-García^{1,2} & Alexander Gusev³

¹ *Instituto de Ingeniería, UNAM, Apdo. Postal 70-472, Coyoacán, 04510 México, D.F.*

² *Centro de Investigación Sísmica, A.C., FJBS, Camino al Ajusco 203, Tlalpan, 14200 México, D.F.*

³ *Instituto de Geofísica, UNAM, Apdo. Postal 70-472, Coyoacán, 04510 México, D.F.*

Received 27 August 1996; accepted in revised form 30 October 1997

Key words: regional amplification, path effects, coda-length, magnitude residual, finite difference, SH waves

Abstract

Seismic ground motion in central Mexico is amplified relative to ground motion observed at the same epicentral distance along the Pacific Coast in a frequency band that includes destructive ground motion at Mexico City. Although several hypothesis have been advanced, at present there is no generally accepted explanation of such amplification. We have analyzed coda-length magnitude data reported by Servicio Sismológico Nacional (SSN) for events recorded during 1993 to increase our understanding of the spatial distribution of this phenomenon. Our results indicate that regional amplification: (a) is detected by magnitude residual computed at each station, relative to the average of SSN network; and (b) is likely related to the crustal structure under the central portion of the Transmexican Volcanic Belt (TMVB). Finally, preliminary wave propagation modelling (using SH wave, finite difference method) suggests that crustal heterogeneity is a possible cause of regional amplification. However, if this is so, it is required that both geometry and velocity distribution vary between the coast and Mexico City.

Introduction

Mexico City may be strongly affected by earthquakes occurring in the subduction zone along the Pacific coast, more than 300 km away. A major factor is local amplification of ground motion generated by a very soft clay layer that covers the lake bed zone of Mexico City (e.g., Bard et al., 1988; Chávez-García and Bard, 1994). However, it has been shown that seismic ground motion on 'firm ground' in the valley of Mexico is already amplified relative to a rock site at the same epicentral distance along a different trajectory (Singh et al., 1988, 1995). This amplification affects a large area in central Mexico, and has therefore been called regional amplification.

In a systematic study of acceleration records from 8 large events of the subduction zone, Ordaz and Singh (1992) quantified the regional amplification. These authors showed that ground motion on firm rock in Mexico City is amplified by a factor up to 10 in the frequency band 0.2 to at least 2 Hz, relative to average

attenuation curves. At 5 Hz, regional amplification has disappeared. Such large amplification was later confirmed by similar analyses using data recorded during a large scale refraction experiment (Cárdenas, 1993).

Significant regional amplification is thus well documented by independent observations. Some hypothesis that have been advanced in the literature are: very large sedimentary valleys (Ordaz and Singh, 1992), lateral heterogeneities in the crustal structure of central Mexico (Chávez-García et al., 1994) and the presence of melted material under the Mexico City valley (Rodríguez et al., 1996). In a recent paper, Shapiro et al. (1997) propose that the hypothesis of Singh et al. (1995), an irregular low-velocity layer under Mexico City valley, explains both the amplification and the increase in duration of ground motion. However, their model does not explain the amplification observed by Ordaz and Singh (1992) in station CUE. In order to confirm the hypothesis of Shapiro et al. (1997) a more detailed knowledge of the spatial distribution of regional amplification is required.

One of the purposes of this paper is to investigate the spatial distribution of regional amplification in central Mexico. According to Ordaz and Singh (1992), regional amplification affects ground motion in a frequency range both below and above a 1 Hz. For this reason, we expect that it may be observed in the short-period (1 Hz seismometers) national network operated by Servicio Sismológico Nacional (SSN). The SSN network has over thirty stations distributed in Southern Mexico, and records several hundreds of events each year. Thus, if it is possible to detect regional amplification in the SSN network, we could have an idea of its geographical distribution. The SSN network, however, has not been calibrated, and its amplitudes are not useful. For this reason, we have explored the possibility of using coda-length magnitude data reported by SSN during 1993. We show that regional amplification is indeed detected by such data, and that this allows us to provide a first estimate of its geographical distribution. Coda-length magnitude data suggest that regional amplification is related to the laterally heterogeneous crustal structure resulting from the presence of the Transmexican Volcanic Belt (TMVB).

The second purpose of this paper is to explore the likely causes of regional amplification. The critical frequency range for Mexico City lies below 0.5 Hz, i.e., frequencies lower than those that can be observed with a short-period network. This suggests that, from the point of view of destructive ground motion in Mexico City, both the important wavelengths and the heterogeneities that affect these waves are large. Besides, although it may be impossible to propose a model of the crust to compute ground motion in the short period range, this is feasible in the long period range. For these reasons, we have explored in this paper SH wave propagation in simple 2D models. The reason we have not tried to construct a model of the real geological structure of central Mexico is that there is not enough data on the shape, nor on the mechanical properties of the crust between the Pacific coast and Mexico City (e.g., Shapiro et al., 1997). Earthquakes in Mexico are located using flat layers models. We have computed results for smooth laterally irregular structures that examine two possible changes to the flat layered structure: continuous lateral velocity changes and slow layer thickness variations. We show that, if crustal heterogeneity is to explain regional amplification, it is required that both velocity distribution and geometry vary between the coast and central Mexico.

Data analysis

Data acquisition

Servicio Sismológico Nacional (SSN) operates the national earthquake observation network. We hypothesized that regional amplification can be detected by this short period (1 Hz seismometers) network. Ordaz and Singh (1992) showed that regional amplification is indeed significant for frequencies as large as 2 Hz. The network is not calibrated, thus it is not useful to make absolute measurements of amplitude data distribution. However, it may be possible to gain insight from relative measurements within the network.

We have chosen to analyze coda-length magnitude (M_c) data, reported in a daily basis by SSN, during 1993. SSN reports M_c for each event, which results from the average of the individual values for all the stations that recorded it. The formula used to compute M_c was proposed by Havskov and Macías (1983) who followed the method of Lee et al. (1972) using data from Mexican stations. This formula is

$$M_c = 0.09 + 1.85 \log_{10}(T) + 0.0004(D), \quad (1)$$

where T is coda-length in seconds and D is epicentral distance in km. The use of this particular equation has little effect in our results, since we will consider only relative differences. We quantify these differences defining the magnitude residual (MR) for each event as the difference between observed magnitude at each station and the reported magnitude for that event.

During 1993 the bulletins of SSN reported data from 34 stations, 30 operated by SSN and 4 (III, IIT, IIA, and IIS) that are part of SISMEMEX, operated by Instituto de Ingeniería, UNAM. All these stations are located on competent rock. Data from seven stations were discarded because they recorded less than 30 events during 1993. As we expect a large scatter, we require enough data to compute a meaningful average MR. From the remaining 27 stations, 9 form the Guerrero subnetwork (GN). This subnetwork has an aperture of 90 km and forms a local array parallel to the coast, 40 km NW of Acapulco (station ACX in Figure 1a). During 1993, GN recorded mainly events from the subduction zone in front of Guerrero, at short epicentral distances, and very few events from the rest of the subduction zone. The station distribution of GN and its recorded data are not at all suited to analyze effects related to propagation along large distances perpendicular to the coast. For this reason, we restricted ourselves to data from the 18 stations shown in Figure 1a.

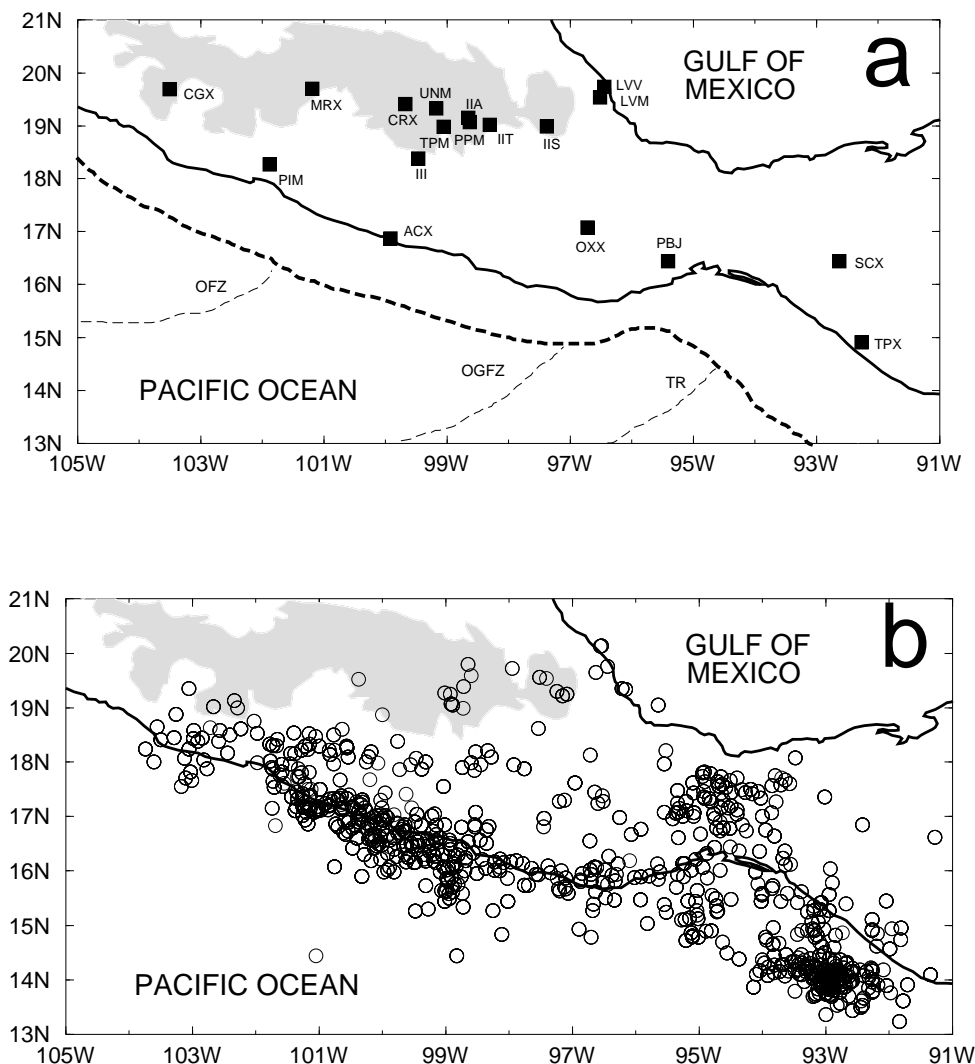


Figure 1. Data used in this study. Solid squares: SSN stations. (a) Distribution of stations of Servicio Sismológico Nacional (SSN). The heavy dotted line shows the location of the trench, while the thin dotted lines indicate fractures of the subducting plate. (b) Location of epicenters recorded by SSN network during 1993. Gray area shows the surface extension of Transmexican Volcanic Belt (TMVB).

Figure 1b shows the distribution of seismicity. A total of 786 events were analyzed. Seismicity occurs mainly along the Mexican subduction zone, with additional activity in the isthmus of Tehuantepec. We analyzed MR at each station for its dependence on four parameters: magnitude and depth of the event, and azimuth and distance between epicenter and station.

MR dependence on magnitude and depth of the events

Recorded events have coda-length magnitude between 2.6 and 5.5. We first investigated whether MR depended on magnitude. An example of the results is shown in

Figure 2. This figure shows that MR does not depend on magnitude of the events for most of the stations (CGX, MRX, UNM, ACX, OXX and TPX). The two exceptions are stations SCX and IIS, where MR decreases with increasing magnitude. Most of the stations show a large uncertainty of the mean for small and large magnitudes. In Figure 3, we plot the data set used to compute the average values of Figure 2. We observe that the large uncertainty of the average value at the lower and upper limits of magnitude values is due to having too few points. This does not explain the large scatter at low magnitudes observed for ACX. This station recorded an unusual number of small magnitude events because

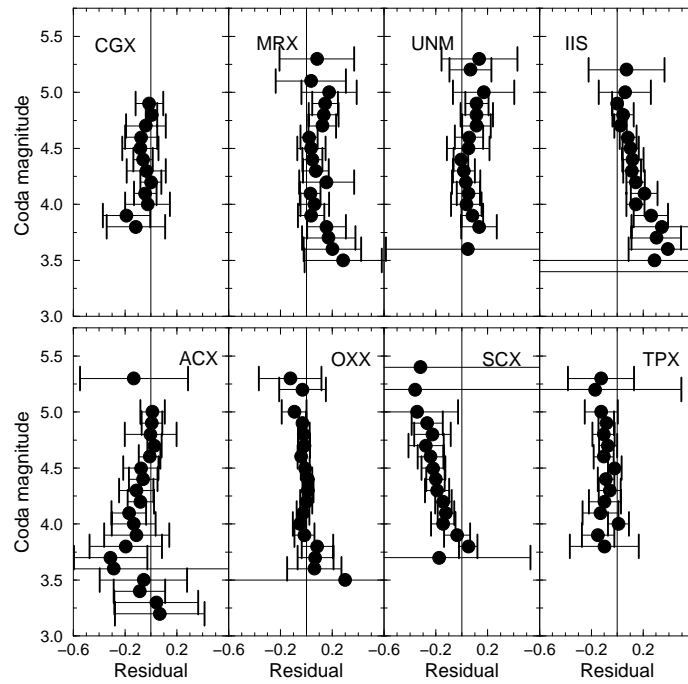


Figure 2. Variation of MR with magnitude for eight stations. Solid circles show average MR for each magnitude. Error bars indicate the 95% confidence limits of the mean. MR for two stations (SCX and IIS) show some dependence on magnitude. The rest of the stations (including those not shown) show MR independent of magnitude of the events.

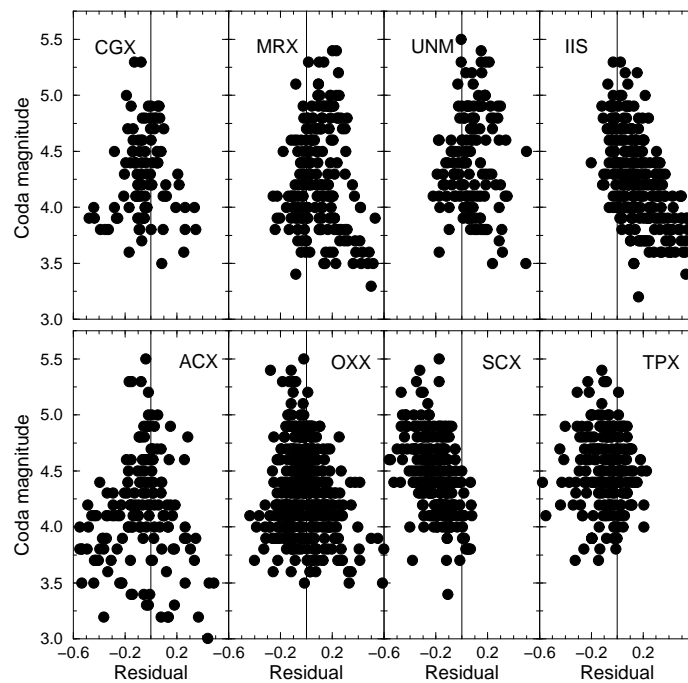


Figure 3. Variation of MR with magnitude for eight stations. Each solid circle corresponds to one event.

of its closeness to the subduction zone. Havskov and Macías (1983) derived its formula without data from epicentral regions and for events of $m_b \geq 4$. Thus, data for ACX may be less reliable than that for the other stations.

We also studied, the possible dependency of MR on the depth of the hypocenter. The depth of our data lies between 0 and almost 200 km. Our results showed that MR does not depend on the depth of the hypocenter for any of the stations (Figure 4).

MR dependence on azimuth between epicenter and station

Next, we considered the possible influence of azimuth between epicenter and station on MR. To evaluate this, we considered for each station those events falling in different azimuth windows (generally 10° wide). Figure 5 shows, for example, these azimuth windows for station UNM.

Our results indicate that for 12 of SSN stations MR does not depend on azimuth between source and station. As regards the remaining stations, 4 of them (MRX, CRX, UNM and IIA, located at the center of the country) present positive MR for epicenters located on the coasts of Oaxaca and Chiapas, while for all the other epicenters, MR is about zero. However, epicenters on the coasts of Oaxaca and Chiapas are those with largest epicentral distance for these stations. In fact, given the geographical distribution of events, azimuth between epicenter and station is coupled to epicentral distance. This is clearly shown in Figure 5 for station UNM. A similar situation is observed at station CGX, for which MR is negative for epicenters in the coast of Michoacán (closer epicentral distance) and about zero for epicenters on the coast of Guerrero (larger epicentral distance) at slightly different azimuths. We conclude then, that the dependence of MR observed for these five stations may not be real, as it may result from a dependence of MR on epicentral distance. This hypothesis is supported by the non-dependence of MR on azimuth for all the other stations, which have a better coverage of the observed ranges for azimuth and distance.

OXX is the only station that shows a clear dependence on azimuth, independently of epicentral distance. For this station, MR is zero in average for events coming from all azimuths except between 150 and 210° (measured counter clockwise from the North), range for which the average MR is negative. Thus, MR is negative for those events occurring in front of the

coast of Oaxaca, and between the coast and the station itself. Negative MR suggests larger than average attenuation. In fact, Q values measured in the coast region of Oaxaca are lower than elsewhere along the subduction zone and have been interpreted as due to a more fractured crust, without tectonic stress accumulated in this region (Castro et al., 1994). Therefore, MR dependence on azimuth for OXX station is probably related to very local phenomena, and unrelated with regional amplification.

MR dependence on epicentral distance

We also analyzed the possible dependence of MR on epicentral distance. It is clear that only larger events are recorded at larger epicentral distances. However, as shown above, no significant dependence of MR on magnitude was observed at most of the stations.

Some results are shown in Figure 6 for the complete data set analyzed at some of the stations. In this plots, MR for stations MRX, CRX, UNM, and TPM, suggests some dependence with increasing distance. For example, for station MRX, MR is positive for all observations at distances larger than 600 km. However, the number of data points at large distances is small and the 95% confidence limits of the average values (not shown) cannot rule out that average values are independent of epicentral distance.

The formula we have used to compute M_c may not be appropriate for the whole distance range we have investigated. However, in this case, we would find the same dependence of M_c with distance for all the stations. Figure 6 suggests that the trend of MR for large epicentral distances is not the same for all the stations (compare MRX with III in Figure 6, for example). Thus, Figure 6 offers some indication that MR increases for large epicentral distances, but only for some stations.

Summary

Given the spatial distribution of our events, we have explored a different grouping of our data. Most of the events occur along the subduction zone. We have divided the subduction zone in four subzones, and analyzed mean and the coefficient of variation (CV) of MR for each station for all the events in each subzone. Each subzone is bounded by fractures of Cocos plate (shown in Figure 1a) and presents different convergence rates between oceanic and continental plates (Pardo and

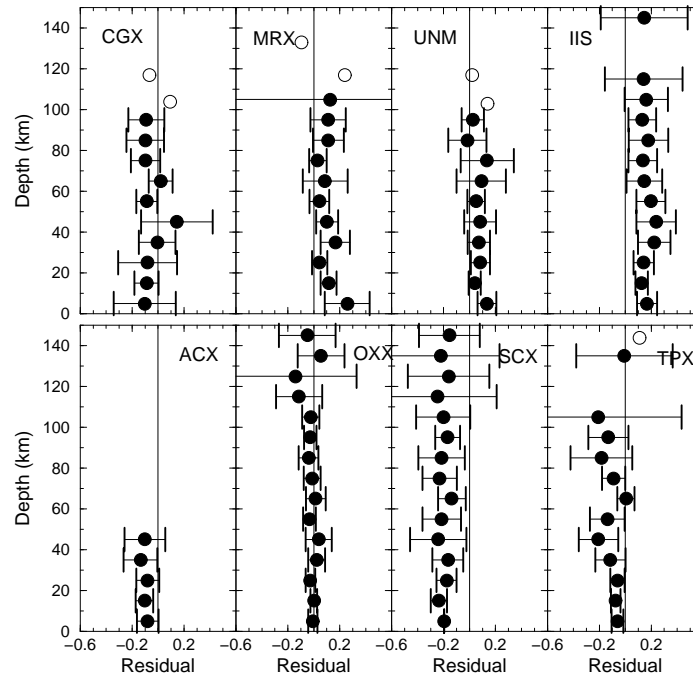


Figure 4. Variation of MR with depth of the events for eight stations. MR is independent of depth of the hypocenters for all the stations used in our study. Solid circles show average MR in a 10 km window. Error bars indicate the 95% confidence limits of the mean. Open circles indicate that only one event was observed in that depth window.

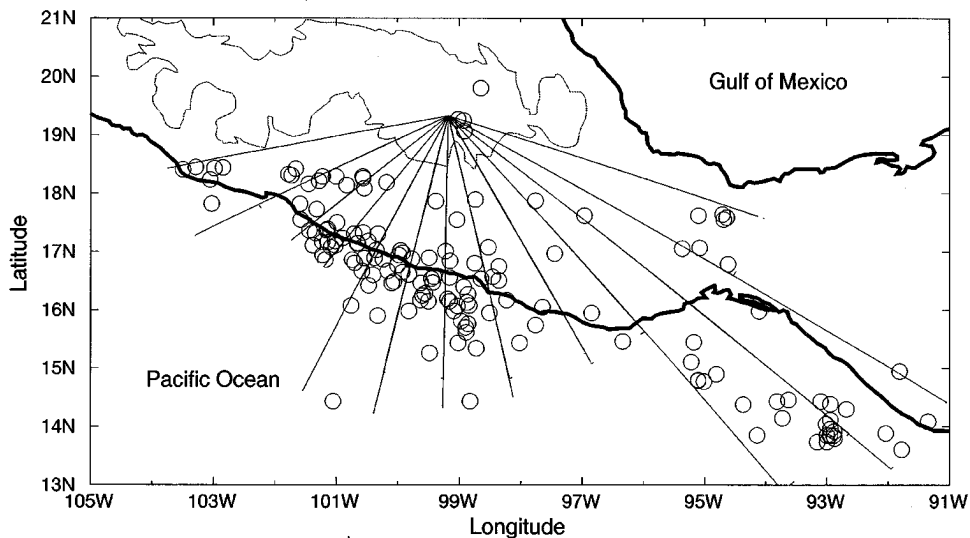


Figure 5. Example of separation of events in azimuth windows. Open circles: epicenters of all of the events recorded by station UNM (located where all the lines converge) during 1993.

Suárez, 1995). Subzone 1 (104° W to 102° W) is bounded by Orozco fracture (OFZ) to the SE. Subzone 2 (102° W to 98° W) is the Guerrero region, the most active of all, bounded to the SE by O'Gorman fracture

(OGFZ). Subzone 3 (98° W to 95° W) is bounded to the SE by Tehuantepec ridge (TR). Finally, subzone 4 extends from 95° W to 91° W, and is the second most active.

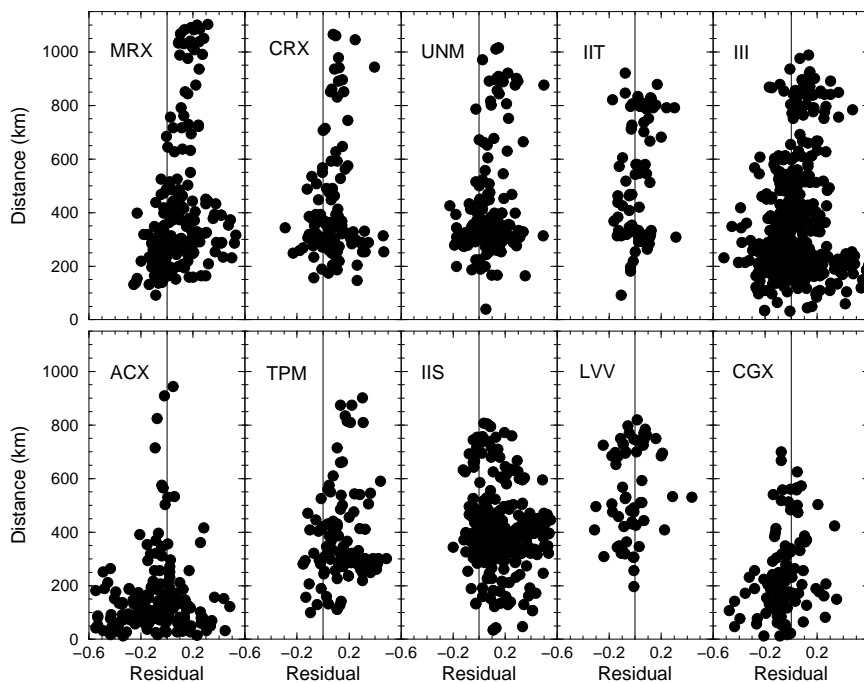


Figure 6. Variation of MR with epicentral distance for ten stations. Each solid circle corresponds to one event.

Figure 7 shows distribution of average MR and its CV for each of the four subzones. Mean and CV for MR were computed for all the events with epicenter within the rectangles shown in each one of the four diagrams. Results for subzone 1 (Figure 7a) show small MR in all the stations except for IIS and PPM. We note that some stations (LVV, LVM, SCX, PBJ, TPX, IIA, and IIT) did not record events from this subzone. MR is positive in the central stretch of TMVB, except for stations CRX and MRX. These two stations are those for which whose epicentral distances are smallest.

Figure 7b shows average MR and its CV for events whose epicenters fall in subzone 2. All the stations in central Mexico show positive with small CV. The largest average value is that of PPM (0.26). Along the Pacific coast, average values are negative for ACX, PIM, and CGX, while they are small and positive to the East of subzone 2 (stations OXX and PBJ).

Results for subzone 3 are shown in Figure 7c. Average MR is positive only at the center of the TMVB. For all the other stations for which CV was less than 2, MR is negative. This applies both for stations along the Pacific coast and for LVV and LVM on the Gulf coast.

Finally, results for subzone 4 are shown in Figure 7d. This figure shows positive average MR in the

TMVB, and negative MR outside it. We note that station PIM, along the Pacific coast did not record any event from subzone 4, while station MRX, at approximately the same epicentral distance, recorded 30 events from subzone 4.

Figure 7 shows that MR is consistently positive in the central stretch of TMVB. Station CGX, on its Western edge shows negative MR (subzones 1, 2, and 3) or too large CV (subzone 4). Outside TMVB, stations OXX and PBJ show positive MR for subzone 2, but negative MR for subzone 3. These results suggest that duration of ground motion is increased relative to average on central TMVB, and decreased along the Pacific coast. The differences between subzones 1 and 2 suggest that this increase in duration is more important when the waves travel obliquely to TMVB than when they travel parallel to it. Regional amplification is about a factor 5 to 7 in the 1–2 Hz frequency band (Ordaz and Singh, 1992). This amplification could increase the measured duration of a weak motion record, and result in a positive MR relative to average. Figure 7 suggests that regional amplification in central Mexico is detected by MR of the short-period SSN network, and that it is related to lateral heterogeneity associated with the TMVB.

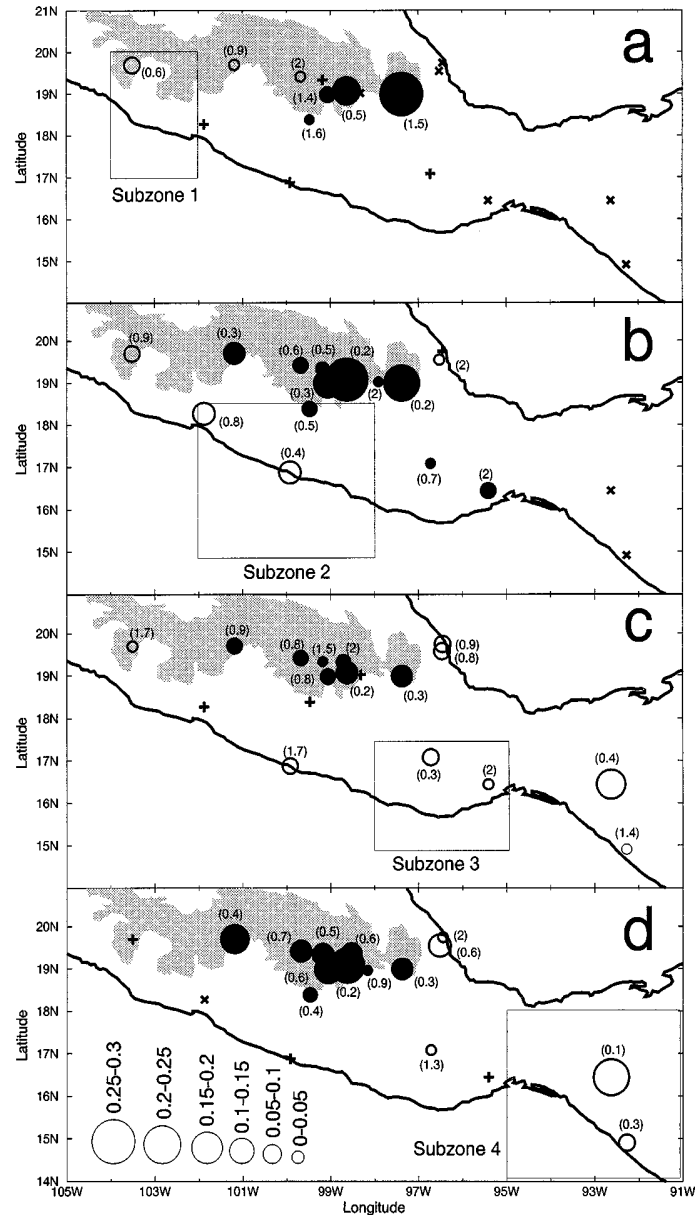


Figure 7. Distribution of average MR values for epicenters coming from each one of the 4 different subzones. The size of the symbol indicates the value range of MR. Solid symbols show positive MR, while open symbols indicate negative MR. The values between parenthesis are the coefficients of variation. Pluses indicate stations where the coefficient of variation was larger than 2. Crosses indicate stations that did not record events from the corresponding subzone.

Preliminary wave propagation modeling

Our results shed some light on the spatial distribution of regional amplification. They allow, for example, to discard the hypothesis of large alluvial valleys because, given the spatial distribution of regional amplification

obtained from MR, this alluvial valley would be too large, and cannot be identified in the geological map of Central Mexico. MR distribution suggests that regional amplification is likely related to the crustal heterogeneity caused by the TMVB (Transmexican Volcanic Belt). However, our results do not have enough resolu-

tion and are insufficient to constrain a model that could explain the observations.

Several studies have investigated crustal structure in Mexico. Valdes et al. (1986) proposed an average velocity model for the zone of Oaxaca. Campillo et al. (1989) modified slightly this model to better explain the relative arrival times of Lg waves and long period Rayleigh waves in Mexico City from the 9.19.85 Michoacán event. Chávez-García et al. (1995) showed that this model allowed to correctly predict the average dispersion curves between 7 and 20 s between the Pacific coast and Mexico City, but some observations suggested that lateral variations could be important.

Additional restrictions on the crustal structure come from gravity data. Two recent models are those of Molina-Garza and Urrutia-Fucugauchi (1994) and Campos-Enríquez and Garduño-Monroy (1995). According to these authors, the thickness of the crust increases from the coast (Pacific Ocean and Gulf of Mexico) towards central Mexico, reaching between 47 km (Molina-Garza and Urrutia-Fucugauchi, 1994) and 38 km (Campos-Enríquez and Garduño-Monroy, 1995) under TMVB. However, both models show an anomaly under the central stretch of the TMVB. Molina-Garza and Urrutia-Fucugauchi (1994) propose a low density layer at the base of the lower crust, which is involved in the isostatic compensation of the volcanic-capped plateau of the TMVB. The top of the anomalous low-density layer is at about 30 km, whereas its base reaches a maximum depth of about 47 km beneath the TMVB. Campos-Enríquez and Garduño-Monroy (1995) suggest that the central part of TMVB is an area of relative thinner crust. This crustal thinning is related to the extensional tectonics affecting, since the Late Miocene, the western and central sectors of the TMVB.

This is still not enough to constrain a seismological model. We have chosen to investigate ground motion in preliminary 2D models. In particular we will examine the influence of two factors: a horizontal velocity gradient between the Pacific coast and Mexico City, and a smooth irregular interface, within the first 30 km of the crust. Thus, we will explore whether regional amplification can be explained by a gradual decrease in propagation velocity, a gradual decrease of the thickness of the layer guiding surface waves, or both together.

Method

We have used the finite difference method to model ground motion, exclusively for SH motion. The pro-

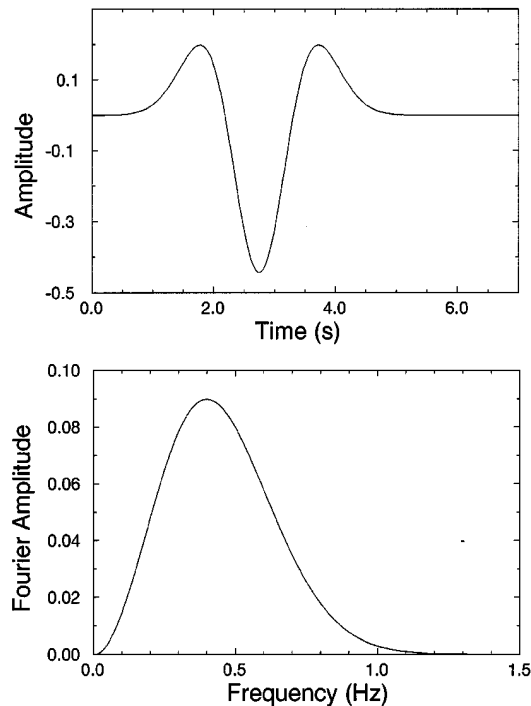


Figure 8. Ricker pulse and amplitude spectrum of the same, used as the time function of the source in finite difference simulations.

gram used was that by Moczo (1989) where the details of the finite difference scheme are given. One point worth mentioning is that Moczo (1989) uses an approximation called ‘heterogeneous formulation’, to rigorously consider discontinuities of the material properties that do not coincide with any grid point. This allows to model accurately continuous lateral variations of velocity and a perfectly smooth irregular interface. The free surface is modelled using the vacuum formalism, and a point source is included following Aboudi (1971). The FD scheme by Moczo (1989) makes it possible to consider anelastic attenuation, following the ideas of Emmerich and Korn (1987). However, as we are only interested in comparing different models, we have neglected anelastic attenuation throughout.

All the models consider a regular grid spacing of 150 m in the horizontal and vertical directions. The models are 450 km large in the horizontal direction and 45 km in the vertical direction. The first 30 km represent the crust. In the half-space the velocity is 4.6 km/s and the density 3.0 g/cm³, both constant for all the models. The upper 30 km of the model include an irregular smooth interface with an exponential shape. Velocity in the upper layer follows a linear gradient

and goes from 3.05 km/s in the left edge of the model down to 2.15 km/s at 450 km. The second irregular layer includes also a velocity gradient, from 4.47 km/s in the left edge down to 3.42 km/s. Thus, velocity contrast between these two layers is kept approximately constant along the profile. Density is the same for the upper 30 km and changes linearly from 2.85 g/cm³ at the left edge down to 2.55 g/cm³ at the right edge of the model. This basic model satisfies the requirement of being, when averaged, the 1D model proposed by Campillo et al. (1989). The source time function we have used for FD computations is a Ricker pulse with a dominant period of 2.5 s (Figure 8). This pulse includes those frequencies that are affected by regional amplification. The source is located 75 km from the left boundary. Mexico City would be at an epicentral distance of about 300 km.

Models

The basic model (model 1) is shown in Figure 9a. It includes the horizontal velocity gradient and an irregular interface dividing the crust in two layers. Two possible source depths have been used in this model: 10 km (model 1A) and 20 km (model 1B). We considered two additional variations for this model. The first one (model 1C) considers constant velocity and density within the two irregular layers (3.05 km/s in the first and 4.3 km/s in the second layer, density is the same in both layers, 2.85 g/cm³). the depth of the source was 10 km. The second variation to the basic model (model 1D) kept the velocity and density gradients, but used an irregular interface with a smoother lateral variation (Figure 9b). The source depth was again 10 km.

The second model (model 2) consists simply of two flat layers, each one 15 km thick. Velocity and density distribution correspond to those of model 1A. This model will allow us to quantify how much amplification is due to the irregular lateral structure of model 1. In model 2 the source depth is 10 km.

Finally, a third model explores the influence of the shape of the irregular interface. In model 3 (Figure 9c), the crust has two flat layers between 0 and 175 km from the edge of the model. From 175 km to the right edge, thickness of the crust decreases slowly to about 20 km at 300 km epicentral distance (roughly corresponding to Mexico City). Velocity and density distribution are the same as those for model 1A in the two irregular layers. Source depth is 10 km.

Results

Figure 10 shows an example of the results. We present synthetic seismograms for some chosen receivers along the free surface of model 1A. At close epicentral distances, direct arrival and some multiples are the only features of the synthetics. For epicentral distances larger than about 100 km, Love waves are established, guided by the topmost layer. At large epicentral distances, body wave arrivals have very small amplitudes, while Love waves form a sharp pulse whose amplitude increases steadily with distance.

One way to compare all the models is to plot together peak ground displacement of the synthetic seismograms (smoothed with a boxcar window 18 km wide) as a function of distance. This is shown in Figure 11. No normalization was applied, as all the traces were obtained with the same source time function. From 0 distance (directly above the point source) to 125 km we observe large variations and a sharp decrease of amplitude due to geometric attenuation of direct arrivals, with some peaks where reflected arrivals become important. At larger epicentral distances we observe different behaviors depending on the model. Model 1A (including the irregular interface and the velocity gradient) shows a peak displacement increasing steadily with distance. This contrasts sharply with results for model 1B, whose only difference with model 1A is a deeper source. Peak displacement for model 1B decreases with distance and has the smallest amplitudes among the models at large distances. Difference between models 1A and 1B is a factor of 3 at 330 km epicentral distance. Results for model 1D (Figure 9b) are similar to that for model 2 (flat layers), suggesting that the smooth irregular interface is not significantly different from a flat interface. Results for model 3 (Figure 9c) and model 1C (including the irregular layer, but with constant velocity) are similar, which indicates that the irregular interface of model 1C amplifies peak ground displacement as much as the lateral velocity gradient and a linear thickness decrease together.

Figure 11 suggests that an important factor in amplitude of motion at large epicentral distances is the distance between the source and the nearest interface. If this distance is small, ground motion will be smaller (models 1B, 1D, and 2); if it is large, ground motion will be larger (models 1A and 1C). In order to understand these differences we analyzed snapshots of ground motion in the models. Figure 12 shows absolute amplitudes of displacement in part of models 1A and 1B, 62 s after onset of the computations. The only dif-

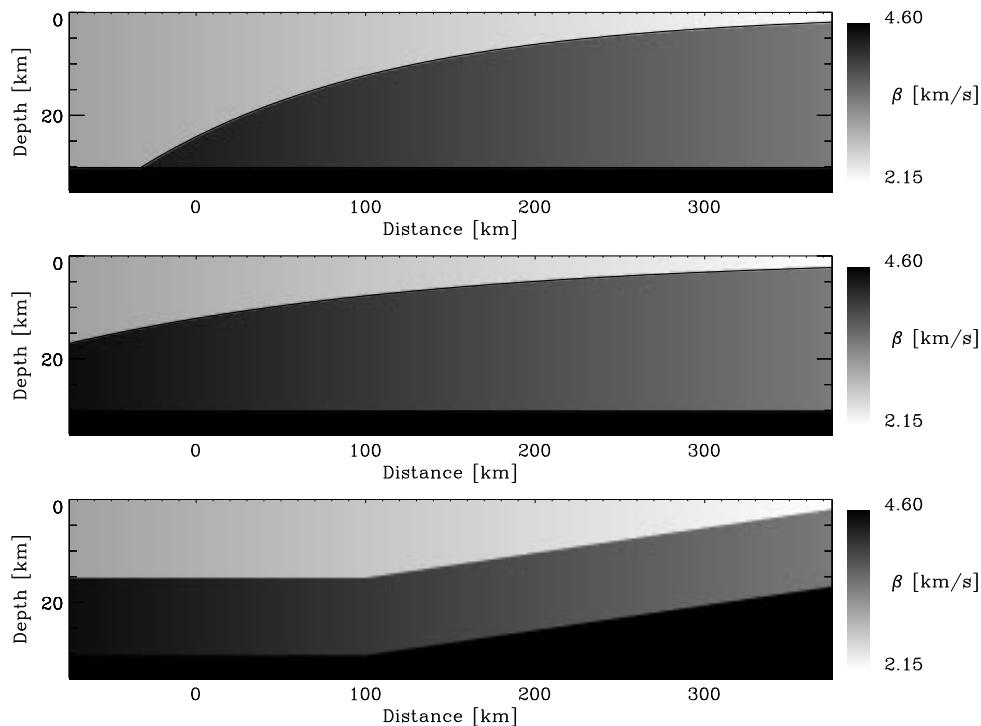


Figure 9. Three of the models used for FD computations. (a) Basic model including lateral velocity and density gradients and an irregular interface (model 1A). (b) Modification of the basic model. Velocity and density structure is the same, but the shape of the irregular interface is smoother (model 1D). (c) Model with a linear decrease in crustal thickness for epicentral distances larger than 175 km (model 3). The star indicates the position of the source. Mexico City would be at about 300 km distance.

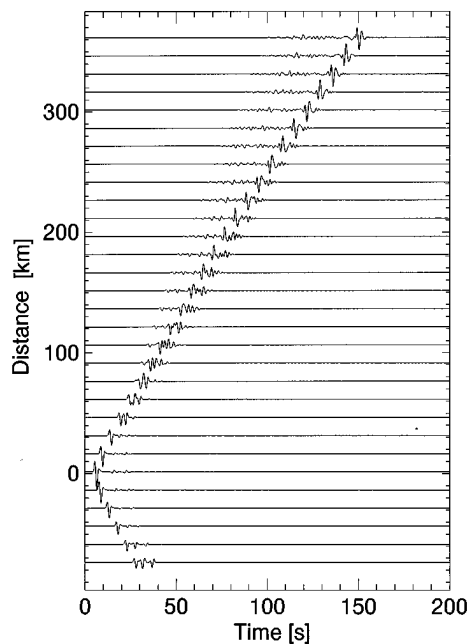


Figure 10. Synthetic seismograms obtained for model 1A.

ference between these two models was the depth of the source. For this time level, Love wave propagation is well established. In model 1B, the largest amplitudes are distributed in several maxima with depth. In contrast, model 1A shows the largest amplitudes at the surface (between 150 and 160 km epicentral distance), decreasing monotonically with depth. Thus, the main difference between these two models is the Love wave mode that has been most excited: the fundamental in the case of model 1A, a higher mode in the case of model 1B.

One interesting feature of observed regional amplification is its frequency dependence. Ordaz and Singh (1992) showed site amplification functions for eight sites in central Mexico from accelerographic data. They computed amplification relative to average attenuation for all the network. We have read these amplification curves (one for each of their eight events) and computed a geometric average for each station. We left out stations CUE and MAD because they recorded only one event, and station TEA because the distance from this station to the source is very different from the

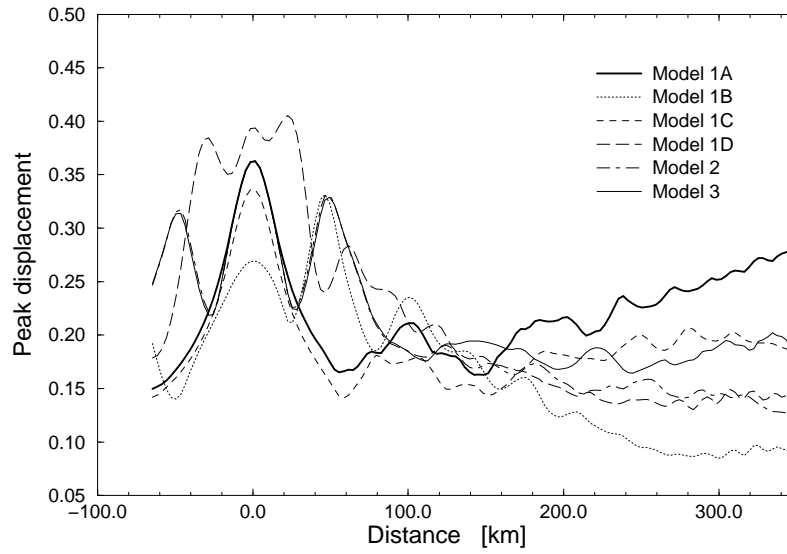


Figure 11. Peak displacement of the synthetics as a function of epicentral distance for all the models.

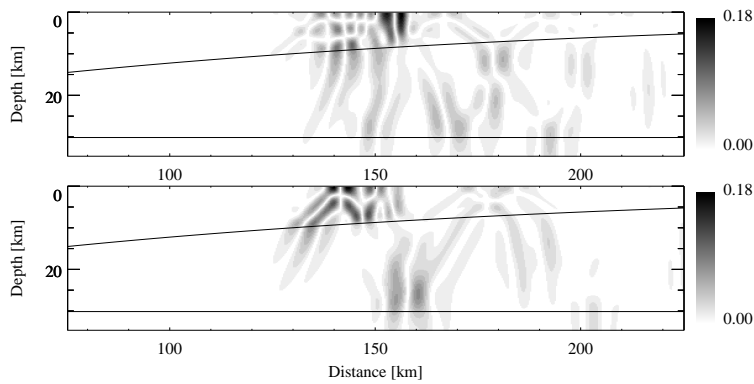


Figure 12. Snapshots for models 1A (upper frame) and 1B (lower frame) at same time level (62 s). The difference between the two is only the depth of the source (10 km for 1A, 20 km for 1B).

Table 1.

Event date (d/m/y)	Depth (km)	Ms	Stations							
			B18	B34	B74	CUE	CUI	MAD	TAC	TEA
19/09/85	16	8.1					×	×	×	×
21/09/85	20	7.6					×		×	×
07/06/87	23	4.8			×					×
08/02/88	20	5.8	×	×	×		×			×
25/04/89	17	6.9	×	×	×		×		×	×
02/05/89	19	4.9		×	×					×
08/10/89	37	4.1					×			
31/05/90	21	5.8	×	×		×	×		×	×

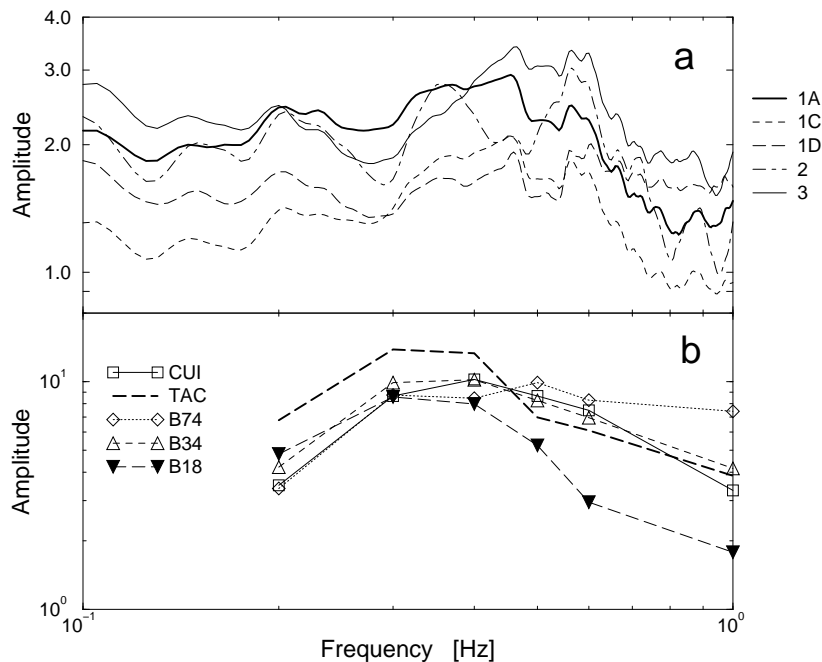


Figure 13. Comparison of the shape of spectral amplification observed in Mexico City with spectral amplification of theoretical models. (a) Observed values, read from the figures of Ordaz and Singh (1992). (b) Theoretical values, computed relative to synthetic motion computed for model 1B.

others. Epicentral distance for all these stations is comprised between 300 and 340 km. Table 1 shows which events were recorded by each station. The resulting average amplification functions for each of the five sites are shown in Figure 13b, in the frequency range 0.2 to 1 Hz. Maximum amplification attains a factor 14 at 0.3 Hz for station TAC. A significant feature of these curves is that, for most of the stations, the largest amplification occurs in a narrow frequency band, between 0.3 and 0.5 Hz. Outside this band, amplification values decay.

We have made a qualitative comparison of these observations with the results of our models. To this end, we computed a theoretical transfer function for each receiver as the spectral ratio of Fourier amplitude spectra between each model and a reference model. We used 1B as reference model 1B, which showed the smallest peak displacement values at large epicentral distances. Before taking the ratio, we have smoothed Fourier amplitudes with a boxcar function of 0.07 Hz width. Given that all the observations shown in Figure 13b are for epicentral distances in the range 300 to 340 km, we averaged our theoretical transfer functions for all of receivers in this distance range. Our results are reliable in the band 0.1 to 0.7 Hz, given the spectrum of

the Ricker wavelet used at the source. Outside this frequency band, the spectral ratio becomes unstable due to the small amplitude of the denominator. The results are shown in Figure 13a. We first note that observed amplification is larger than predicted. While observed amplification attains a factor 10 in average for all the stations, our theoretical transfer functions have much smaller values, between 2 and 4. However, there is a definite similarity in the shape of both sets of curves. Theoretical transfer functions show maximum amplification in the frequency band from 0.3 to 0.6 Hz, with a decay of amplification outside this band. The amplification decay at low frequency, however, is slower than observed. Another difference is that maximum amplification is shifted towards higher frequencies in the theoretical transfer functions, relative to observed.

Conclusions

Different studies have demonstrated the existence of significant regional amplification of seismic ground motion in central Mexico. Its amplitude as well as the frequency band in which it appears make regional amplification an important factor of the seismic hazard

that threatens several large cities in central Mexico, including Mexico City.

In this paper, we have analyzed coda-length magnitude data reported by Servicio Sismológico Nacional (SSN) for events recorded during 1993. Our purpose was to increase our understanding of the spatial distribution of regional amplification. We analyzed a magnitude residual (MR) defined as the difference between the magnitude computed for a given station-event pair and the magnitude assigned to that event. The latter was computed by SSN as the average of the magnitude estimates from each individual station. We showed that MR does not depend on magnitude (in the range 2.6 to 5.5), depth of the event (in the range 0 to 150 km), nor on azimuth between epicenter and station. MR shows a slight positive dependence on epicentral distance for the stations located on the Transmexican Volcanic Belt (TMVB). MR in the central stretch of TMVB is consistently positive. Our results indicate that regional amplification is detected by MR, and that it is related to the crustal structure under the central portion of TMVB.

We also investigated SH wave propagation due to a point source in several preliminary models of the crustal structure in central Mexico. These models were constructed taking into consideration available data. We investigated the effect on ground motion of a lateral velocity gradient and smoothly varying interfaces. We neglected inelastic attenuation throughout. However, Castro et al. (1994) pointed out the similarity between the Q values determined along the Pacific coast and those determined perpendicular to the coast by Ordaz and Singh (1992). If Q is similar for trajectories parallel and perpendicular to the coast, our relative measurements will not change. We showed that an important factor in the models was the closeness of the source to the irregular interface, that determines which modes of surface waves are excited. Singh et al. (1988) mentioned the depth of the source as a possible factor behind the difference in amplification of ground motion observed in Mexico City between the September 1985 mainshock ($M_S = 8.1$, 16 km deep) and its largest aftershock ($M_S = 7.6$, 20 km deep). Thus, our results suggest that the hypocenter of the 09/21/85 aftershock may have been closer than the mainshock to an irregular interface which would lie at more than 20 km depth on the Pacific coast. An interesting result was that frequency dependence of amplification in our models is similar to observed frequency dependence in strong ground motion (Ordaz and Singh, 1992).

Our results show that crustal heterogeneity is a possible cause of regional amplification. However, if this is so, it is required that both geometry and velocity distribution vary between the coast and Mexico City. Our models are able to reproduce the observed dependence of amplification on frequency. However, observed amplification values are larger than predicted by our model. This may indicate that our models are too simple (for example, P-SV analysis is required). It is clear that additional data is necessary on the crustal structure in central Mexico and that this will be important to further understand regional amplification.

Acknowledgements

Servicio Sismológico Nacional provided duration data of 1993 events. P. Moczo facilitated his finite difference modelling program. The critical reading of M. Ordaz and of an anonymous reviewer greatly improved the manuscript. Finite difference computations were carried out on the Cray Y4MP at DGSCA, UNAM. Part of this research was financed by Cray Research Inc., contract SC-005296, and by CONACYT, contract 400325-5-2405PT.

References

- Aboudi, J., 1971, Numerical simulation of seismic sources, *Geophysics* **36**, 810–821.
- Bard, P.-Y., Campillo, M., Chávez-García, F. J. and Sánchez-Sesma, F. J., 1988, A theoretical investigation of large- and small-scale amplification effects in the Mexico City valley, *Earthquake Spectra* **4**, 609–633.
- Campillo, M., Gariel, J. C., Aki, K. and Sánchez-Sesma, F. J., 1989, Destructive ground motion in Mexico City: source, path, and site effects during the great 1985 Michoacán earthquake, *Bull. Seism. Soc. Am.* **79**, 1718–1735.
- Campos-Enríquez, J. O. and Garduño-Monroy, V. H., 1995, Los Azufres silicic center (Mexico): inference of caldera structural elements from gravity, aeromagnetic, and geoelectric data, *J. Volcanol. Geotherm. Res.* **67**, 123–152.
- Cárdenas, M., 1993, *La atenuación sísmica entre las costas del Pacífico y el Distrito Federal*, Bsc Thesis, Facultad de Ingeniería, UNAM, 37 pp.
- Castro, R. R., Munguía, L., Rebollar, C. J. and Acosta, J. G., 1994, A comparative analysis of the quality factor Q for the regions of Guerrero and Oaxaca, Mexico, *Geoffs. Int.* **33**, 373–383.
- Chávez-García, F. J. and Bard, P.-Y., 1994, Site effects in Mexico City eight years after the September 1985 Michoacán earthquakes, *Soil Dyn. & Earthq. Eng.* **13**, 229–247.
- Chávez-García, F. J., Sánchez-Sesma, F. J., Campillo, M. and Bard, P. Y., 1994, El terremoto de Michoacán de septiembre de 1985: efectos de fuente, trayecto y sitio, *Física de la Tierra* **6**, 157–200.

- Chávez-García, F. J., Ramos-Martínez, J. and Romero-Jiménez, E., 1995, Surface-wave dispersion analysis in Mexico City, *Bull. Seism. Soc. Am.* **85**, 1116–1126.
- Emmerich, H. and Korn, M., 1987, Incorporation of attenuation into time-domain computations of seismic wave fields, *Geophysics* **52**, 1252–1264.
- Havskov, J. and Macías, M., 1983, A coda-length magnitude scale for some Mexican stations, *Geofís. Int.* **22**, 205–213.
- Lee, W. H. K., Benett, R. E. and Meagher, K. L., 1972, A method for estimating magnitude of local earthquakes from signal duration. U.S.G.S. *Open File Report*.
- Moczó, P., 1989, Finite difference technique for SH-waves in 2-D media using irregular grid. Application to the seismic response problem, *Geophys. J. Int.* **99**, 321–329.
- Molina-Garza, R. and Urrutia-Fucugauchi, J., 1994, Deep crustal structure of central Mexico derived from interpretation of bouguer gravity anomaly data, *J. Geodynamics* **17**, 181–201.
- Ordaz, M. and Singh, S. K., 1992, Source spectra and spectral attenuation of seismic waves from Mexican earthquakes, and evidence of amplification in the hill zone of Mexico City, *Bull. Seism. Soc. Am.* **82**, 24–43.
- Pardo, M. and Suárez, G., 1995, Shape of the subducted Rivera and Cocos plates in Southern Mexico: seismic and tectonic implications, *J. Geophys. Res.* **100**, 12357–12373.
- Rodríguez, M., Campos-Enríquez, J. O. and Nava, E., 1996, Seismic attenuation, gravity, and crustal structure under the basin of Mexico, *Geophys. Res. Lett.*, submitted.
- Shapiro, N. M., Campillo, M., Paul, A., Singh, S. K., Jongmans, D. and Sánchez-Sesma, F. J., 1997, Surface-wave propagation across the Mexican Volcanic Belt and the origin of the long-period seismic-wave amplification in the Valley of Mexico, *Geophys. J. Int.* **128**, 151–166.
- Singh, S. K., Mena, E. and Castro, R., 1988, Some aspects of the source characteristics and ground motion amplification in and near Mexico City from acceleration data of the September, 1985, Michoacán, Mexico earthquakes, *Bull. Seism. Soc. Am.* **78**, 451–477.
- Singh, S. K., Quaas, R., Ordaz, M., Mooser, F., Almora, D., Torres, M. and Vásquez, R., 1995, Is there truly a 'hard' rock site in the Valley of Mexico?, *Geophys. Res. Lett.* **22**, 481–484.
- Valdes, M. C., Mooney, W. D., Singh, S. K., Meyer, R. P., Lomnitz, C., Luetgert, J. H., Helsley, C. E., Lewis, B. T. R. and Mena, M., 1986, Crustal structure of Oaxaca, Mexico, from seismic refraction measurements, *Bull. Seism. Soc. Am.* **76**, 547–563.